Presented by:
North American Die Casting Association

Simulation of Flow Pattern and Temperature Profile in the Shot Sleeve of a High Pressure Die Casting Process

L. Wang, T. Nguyen & M. Murray
CSIRO Manufacturing Science and Technology
Melbourn, Vicoria, Australia

Abstract

Air entrapment in the shot sleeve of a high pressure die casting machine is a potential problem that can adversely affect the production of sound castings. Air in the shot sleeve can be entrapped during metal pouring and plunger advancement. A high plunger speed can create surface wave rollover and a low speed can create wave reflections. Both cases can cause air entrapment. This paper analyzes a typical industrial case and presents a 3-D coupled fluid flow and heat transfer simulation to predict the flow pattern and temperature profile during metal pouring into the shot sleeve and the subsequent plunger advancement. It shows that the first metal is splashed within the shot sleeve and quickly loses its temperature. A wave reflection is created as the plunger advances and it causes a metal splash at the sleeve exit. From the result of the flow prediction, an optimum plunger operation is recommended. The thermal analysis predicts that a solid layer forms on the bottom face of the shot sleeve in areas close to the die.

Introduction

In the cold chamber process of high pressure die casting (HPDC), molten aluminum is poured into a shot sleeve and the plunger pushes the molten metal through a runner and a gate into a cavity. Air in the shot sleeve and in the cavity can be entrapped within the metal due to the highly turbulent flow involved. The entrapped air will remain in the solidified casting in the form of gas porosity, which has an adverse effect on the mechanical properties of the castings.

It is commonly believed that the air in the shot sleeve can be entrapped during the metal pouring (ladling) and the plunger advancement. To minimize the air entrapment during the ladling, a common practice in the foundry is to let the metal settle for one to two seconds after the ladling is complete. This is to allow any entrapped air to escape from the metal before the plunger starts to move.

The second way air can be entrapped is during movement of the plunger. Since the horizontal shot sleeve design prevents complete filling, the advancement of the plunger will create a wave. It has been reported that a high plunger speed can create wave rollover and a low speed can create wave reflections.[1,2] Both cases can cause air entrapment. To avoid these wave problems, the injection process may be divided into multi-speed stages, particularly for modern machines. However, most of the high pressure die casting machines currently serving in the industry can only run two stages, i.e., a low speed stage and a high speed stage (called first speed and second speed, respectively). As far as the air entrapment in the shot sleeve is concerned, the first stage is very crucial. This is because during the second stage the shot sleeve is already full, and little, if anything, can be done to remove any entrapped air.

Air entrapment is not the only problem that can arise in the shot sleeve. Another issue is the solidification of metal in the shot sleeve. Since the temperature of the shot sleeve is generally about 200°C and molten aluminum alloy starts to solidify at approximately 570°C, a chill layer is rapidly forming as the molten metal touches the cold shot sleeve. This solid layer (called cold flakes) can cause problems such as gate blockage during the cavity filling and fracture into the casting at the gate location during trimming.[3]

A number of experimental and modeling studies on the fluid flow in the shot sleeve have been reported.[1,2,4-6] Sheptak (1963)[1] first demonstrated the flow pattern in the slot sleeve with a water analogy. The air entrapment caused by a rollover wave was observed under all the tested conditions with the plunger speeds between 1.27 to 3.05 m/sec. Garber (1982)[2] first developed a mathematical model based on a Bernoulli equation to predict the wave shape in the shot sleeve during the plunger advancement. It was found that there existed a critical speed. When the plunger speed was greater than this critical speed, air entrapment would occur due to the formation of a rollover wave. When the plunger speed was lower than the critical speed, air entrapment could also occur, but this time because the surge wave would run ahead of the advancing plunger, hit the end wall of the shot sleeve

and reflect back. The wave speed, and hence the critical velocity, depended not only on the plunger speed, but also on the shot sleeve diameter and the initial fill level of the shot sleeve. Garber worked out a criterion for the critical velocity for various shot sleeve diameters and initial fill levels. This work became a benchmark for later studies and was implemented into the foundry operations. Brevick and his co-workers (1991)[5] demonstrated with their water analog modeling that the acceleration of the plunger to reach the critical velocity was also important. Bennett (1987)[4] found that a high pouring rate created turbulence during the metal pouring into the shot sleeve. Kuo and Hwang (1998)[6] developed a 3-D model to simulate the flow patterns in the shot sleeve. The SOLA-MAC technique was used in their model to track the free surface and VSEM (Variable Spacing Even Mesh) meshing technique to handle the moving boundary problem. The predicted results were verified by water analog experiments.

In reviewing the previous work, the following points can be made:

- None of the models considered heat transfer in the shot sleeve. In reality, the metal temperature (initially 650-700°C) drops very rapidly once it touches the cold shot sleeve (normally about 200°C). As the metal begins to freeze, its effective viscosity increases dramatically. This will again affect the flow pattern.
- All of the models assumed that the metal was stationary before the plunger started to move and ignored the flow created by pouring the metal into the shot sleeve.
- The analytical models[2,7] derived from the Bernoulli equation oversimplified the real problem. For instance, the viscosity and surface tension of the metal were ignored. These models were limited to the prediction of a simple form of wave in front of the plunger tip. They were not suitable for the cases of wave rollover and reflection. Garber's model is only applicable when the fill percentage is greater than 50%. However, quite often in the foundry the fill percentage is less than 50%.
- The 3-D numerical model by Kuo[6] simulated only the cases with constant plunger speeds. As demonstrated by Brevick's experiments, the acceleration of the plunger from the stationary state to the first stage is also important to the wave formation and propagation.

This paper presents 3-D simulations of heat and fluid flow in the shot sleeve with each of the above factors being included. A typical case from a foundry has been analyzed and optimized.

The Model

The commercial flow simulation package, Flow3D[8], was used in this study. The standard Navier-Stokes equation and the two-equation k-ε turbulence model were employed for the flow simulation. The molten metal was considered an incompressible fluid and the air phase was ignored.

The physical properties of the aluminum alloy selected in this paper are listed in table 1.

Table 1

The geometry of the shot sleeve used in this study is schematically shown in figure 1. The inner diameter of the shot sleeve is 100mm and the distance from the tip of the plunger to the end of the shot sleeve is 620mm.

Figure 1

The plunger speed and displacement under a normal condition, together with those under an optimized condition are illustrated in figure 2. In the first six seconds, the molten metal was poured into the shot sleeve up to 35% of the volume. The normal condition was defined as follows. After a typical one second delay the plunger started to move and was accelerated at a constant rate such that the first speed of 0.25m/sec was reached after 0.1sec. When the piston was at the position where the shot sleeve was full of metal, it was accelerated at a constant rate to the second speed of 2.0m/sec within 0.02 sec. Once the runner and cavity were filled, the piston was stopped at 40mm from the end of the shot sleeve, which is a position resulting in a 40mm thick biscuit in the real casting process. All of those values are close to the parameters currently running in an industrial machine. The technique for optimization is discussed below.

Figure 2

The metal temperature at the inlet of the pouring hole was set to 650°C and the shot sleeve was assigned a uniform temperature of 200°C. The heat transfer coefficient between the metal and the shot sleeve was 4560 W/m^{2}K. This value has been obtained from an inverse calculation based on the data from the thermocouples embedded in the shot sleeve under a similar condition.[15]

Since the geometry and the boundary conditions are symmetrical on the vertical plane passing through the axis of the shot sleeve, only half of the shot sleeve has been simulated.

Flow Pattern

Starting with the metal ladling into the shot sleeve, the following flow patterns and temperature distributions were obtained.

Metal pouring and settling

The predicted flow pattern during metal pouring is shown in figure 3. The color in these images represents the magnitude of the velocity. As illustrated in the image at t=1sec, when the metal is poured into the shot sleeve, it splashes and flows very rapidly along the axial direction of the shot sleeve. When it reaches the end wall of the shot sleeve, it loses momentum and is built up against the walls. The metal level is determined by the incoming metal velocity. As more metal is poured in, a wave is formed and travels back from the far end of the shot sleeve toward the pouring hole. After the ladling is complete, the metal flow gradually settles down. As shown in the last two images in figure 3, the maximum velocity of the metal in the shot sleeve is reduced from the initial 50cm/sec (t=6.0sec) to 15cm/sec (t=7.0sec). This suggests that one second of settlement time is sufficient to achieve flow stabilization.

Figure 3

The same simulation result has also been output for the temperature distribution in a 2-D view on the symmetrical plane in figure 4, which provides an alternative view for the flow pattern. The temperature distribution will be discussed in the later section.

Figure 4

Plunger advancement

The wave formation and propagation during the plunger advancement under the normal condition is shown in figure 5. Again, the color in these images represents the magnitude of the velocity. The dimensional scaling in these images varies, so that, as the plunger advances and the length of the molten metal becomes small, the images are scaled up in order to give a better view of the wave front. These images together with the temperature profile on the symmetry plane are also illustrated in figure 6. By analyzing the wave front positions from the outputs for all the time steps (of which only some are shown in figure 6), the wave travelling speed has been determined and is plotted in figure 7 together with the plunger speed.

Figure 5

Combining figure 5 (3-D view) and figure 6 (2-D view) with figure 7, the following can be inferred: When the plunger is accelerated from the stationary (t=7.0sec) to the first stage speed (t=7.1sec), the molten metal in front of the plunger tip is correspondingly accelerated and a wave is created. As the plunger reaches the first stage speed and keeps advancing at 0.25m/sec, the wave maintains the acceleration for another 0.1second to reach a speed of 0.6m/sec, which is much faster than the plunger speed (as shown in figure 7). After that, even though the acceleration of the wave is reduced, the wave speed continues to increase up to 0.85 m/sec at the time when it hits the end wall. Once the wave hits the wall (t=8.0sec as shown in figures 5 and 6), some of the metal is splashed out through the sleeve exit to the runner. At the same time, the wave is reflected back toward the piston. When the reflected wave meets the moving piston, a new wave touching the shot sleeve ceiling is formed and moves forward in front of the plunger tip.

Figure 6

It is understood that both the wave rollover and wave reflection are undesirable as they can cause metal splashing. This splashing could be a potential problem for the air entrapment. The entrapment severity will depend on whether the splashed metal blocks the gate or not. If the gate is blocked, the air behind the splashed metal may be isolated from the cavity and will be entrapped in the metal. If the splashed metal falls back to the shot sleeve and leaves the gate open, this would not cause an air entrapment problem.

Figure 7

Plunger speed optimization

To avoid the wave reflection, the first wave must touch the ceiling of the shot sleeve. This means that an ideal flow pattern during the plunger advancement may be the one that creates a first wave that touches the ceiling of the shot sleeve and at the same time does not roll over. This is very difficult to achieve when the metal level in the shot sleeve is low. To obtain a certain height of wave touching the ceiling, the plunger must be run with a high speed. A high plunger speed will result in a high wave speed, which is prone to a wave rollover. If the plunger speed is reduced, the first wave cannot touch the ceiling. When this occurs, the wave speed is greater than the plunger speed, as shown in figure 7, and a wave reflection will occur. So, it is very difficult to meet both criteria when the metal level is low in the shot sleeve.

It is found from figure 7 that the first wave speed is determined not only by the plunger speed, but also by the acceleration. A strategy to optimize the plunger operation is to reduce the plunger acceleration rate between the initial state and the first speed stage and also to increase the first stage speed. As the acceleration rate is reduced, the wave speed is also reduced. This slows down the wave to have longer time before hitting the end wall. As the acceleration time is extended, the first wave has more chance to touch the sleeve ceiling since the metal reaches a higher level.

A series of cases with varying acceleration time and the first plunger speed have been simulated. An optimum condition is found to be the one as listed in figure 2. The acceleration time is extended to 0.6sec rather than 0.1sec under the normal condition. Also, the first stage speed is increased to 0.8m/s from the normal 0.25m/s. A higher first speed is necessary. This is because it helps to achieve a greater wave height to touch the ceiling wall. On the other hand, the plunger should move at a higher speed to keep up with the wave. As shown in figure 7, the developed wave speed is about 0.8m/s in the first stage.

Figure 8

The predicted wave formation for the optimized condition is shown in figure 8. During the acceleration stage up to 7.6 sec, a wave is gradually developed in front of the plunger tip. As the wave passes the pouring hole and almost touches the ceiling wall, the plunger moves at the same speed as the wave. This has minimized the time and space to develop a wave reflection.

Temperature Profile

The calculated temperature profiles of the metal in the shot sleeve under the normal condition are shown in figures 4, 6 and 9. The temperature traces at three typical locations (called "probes" in Flow3D) are illustrated in figure 10. The locations of these probes are on the symmetry plane and 2.5mm above the bottom face of the shot sleeve. One probe is under the pouring hole, one in the middle of the shot sleeve and one 70 mm from the sleeve exit.

Figure 9

The temperature profile during the ladling is shown in figure 6. The temperature range in this legend is set to be from the alloy solidus (560°C) to the metal pouring temperature (650°C). As shown in the images, the first metal loses its temperature very fast as it touches the shot sleeve and splashes. The temperature drops about 50°C as the metal gets to the other end of the shot sleeve. This can be seen in figure 10 at t=0.75sec. In the position of 70mm from the exit, the metal temperature drops below the solidus temperature at t=5.5sec. This means that a thin solid layer of the metal starts to form during metal ladling.

Figure 10

The temperature profiles during the first speed and second speed stages for the normal condition are shown in figure 7 and figure 9, respectively. The temperature legend in these figures has been changed to be in the range from solidus

to liquidus (560 to 570°C). It is shown in figure 7 that the majority of the metal is liquid during the first stage and the mushy metal is residing near the bottom face of the shot sleeve. This is because most of the heat is lost from the bottom part of the shot sleeve. As the plunger advances, the liquid metal has more chance to be pushed out to the runner because of its lower viscosity than the mushy metal. As a result, more mushy metal is built up in front of the plunger tip. At the end of the plunger injection, the metal in the biscuit is dominated by the mushy metal and some solids (see figure 9). It is also interesting to see in figure 10 that the temperature in the position of 70mm from the exit is increased during the second stage (after t=8.66sec). This indicates that the solid layer is partially remelted by the hot metal during the second stage.

Where does the first metal go?

Since the first metal from the ladle normally contains more oxides from the pouring ladle and is also the first to react with the tip oil in the shot sleeve, this part of the metal is considered to be poor in quality. It may have a greater probability of generating defects related to metal quality. Therefore, it is interesting to know where the first metal goes. To track the first metal, 3000 "marker particles" were initially positioned in thin layers across the pouring hole. These markers were massless and therefore had no effect on the modeled flow pattern.

The positions of all the markers at different time steps are projected on the symmetry plane and illustrated in figure 11. As the first metal enters the shot sleeve, it is split into two parts, one part being pushed toward the far end and the other part being swirling at the corner of the piston during the metal pouring. As the plunger advances, the majority of the particles stay in the lower part of the metal at some distance from the sleeve exit. During the second stage, some of the particles are squeezed into the cavity and the rest remains in the biscuit.

Figure 11

Conclusions

A 3-D coupled fluid flow and heat transfer simulation has been performed to predict the flow pattern and solidification of aluminum alloy in the shot sleeve of a cold chamber high pressure die casting machine. The simulation shows that:

1) When the metal is poured into the shot sleeve, it flows rapidly along the axial direction of the shot sleeve. By the time it reaches the other end, its temperature has dropped by about 50°C. As more metal is poured in, a wave is formed at the far end of the shot sleeve and travels back toward the pouring hole.

2) After the metal ladling is complete, the enforced flow gradually disappears and a chill layer of solid metal is formed on the bottom face of the shot sleeve. One second of shot delay is sufficient to stabilize the metal flow created by the ladling.

3) In this case of the initial 35% fill percentage (volume), the first wave created by the plunger advancement at the first stage travels faster than the plunger. It reaches the end wall of the shot sleeve, is reflected back, meets the incoming piston and forms a second wave. When the first wave reaches the end wall, metal splashing is generated. Some of the splashed metal escapes from the shot sleeve to the runner. This may be a potential problem to partially block the runner and the gate.

4) The acceleration of the plunger from the stationary to the first stage is important to control the speed of the first wave. A slower acceleration and a higher first speed are preferable to achieve a better wave formation for less air entrapment.

References

1. Sheptak, N. (1963) "Water Analog Study of Fluid Flow in the Cold Chamber." AFS Transactions, 71, 399-404.
2. Garber, L.W. (1982) "Theoretical Analysis and Experimental Observation of Air Entrapment During Cold Chamber Filling." Die Casting Engineer, 26(May-June), 14-22.
3. Gershenzon, M., Rohan, P., Murray M. (1999) "Formation of Cold Flakes in Aluminium High Pressure Die Casting," 20th International Die Casting Congress, Cleveland, Ohio, 305-315.
4. Bennett, C. H. (1987) "Clear Plastic Model Experiments — Cold Chamber Injection Analysis," SDCE 14th International Die Casting Congress and Exposition, Toronto, Ontario, Canada, 1-7.
5. Brevick, J. R., Duran, M., Karni, Y. (1991) "Experimental Determination of Slow Shot Velocity-Position Profile to Minimise Air Entrapment," 16th International Die Casting Congress & Exposition, 399-404.
6. Kuo J. H., Hwang, W. S. (1998) "Flow Pattern Simulation in Shot Sleeve During Injection of Diecasting," AFS Transactions, 106, 497-503.
7. Thome, M. C., Brevick, J. R. (1993) "Modelling Fluid Flow in Horizontal Cold Chamber Diecasting Shot Sleeves," AFS Transactions, 101, 343-348.
8. Flow3D manual, version 7.7, 2001.
9. Bäckerud, L., Chai, G., Tamminen, J. (1986-1990). Solidification Characteristics of Aluminium Alloys, Volume 2, Foundry Alloys, AFS/SKANALUMINIUM.
10. Wang, Q., Davidson, C. (2001). Journal Mater. Sci., 36, 739-750.
11. Magnusson T. (2000). Thesis, Norwegian University of Science and Technology, Trondheim, Norway.
12. Pehlke, R. D., Jeyarajan, A., Wada, H. (1982). Summary of Thermal Properties of Casting Alloys and Mold Materials, Ann Arbor, MI.
13. Perkins, N.D., Bain, C.J. (1965) "Transparent, Water Models as an Aid to Gating Design for Permanent Mold Aluminium Alloy Castings," Journal of Australian Institute of Metals, 10(2), 160-168.
14. Chu Y. L. et al, (1997) "A Study of the Cast Alloy Die Surface Interactions in Aluminium Die Casting," 19th International Die Casting Congress, Minneapolis, Minnesota, T97-075.
15. Hoadley A. (1997). Technical note, CMST CSIRO, Australia.

Parameters	Values	Reference
Liquidus Temperature, T_L, °C	570	9
Solidus Temperature, T_S, °C	560	9
Latent Heat, kJ/kg	495	10
Viscosity, μ, Pas	0.001(1+100 f_s) where solid fraction f_s is proportional to the temperature change in the mushy zone	
Molten metal density, kg/m^3	2430	11
Solid metal density, kg/m^3	2550 (at temperature > 500°C)	11
Molten metal specific heat, J/kg·K	1100	12
Solid metal specific heat, J/kg·K	1050	12
Molten metal thermal conductivity, W/m·K	100	12
Solid metal thermal conductivity, W/m·K	150	12
Surface Tension, N/m	0.84	13
Contact angle between Al and steel, degrees	131°	14

Table 1 – *Physical properties of aluminum alloy used in this simulation.*

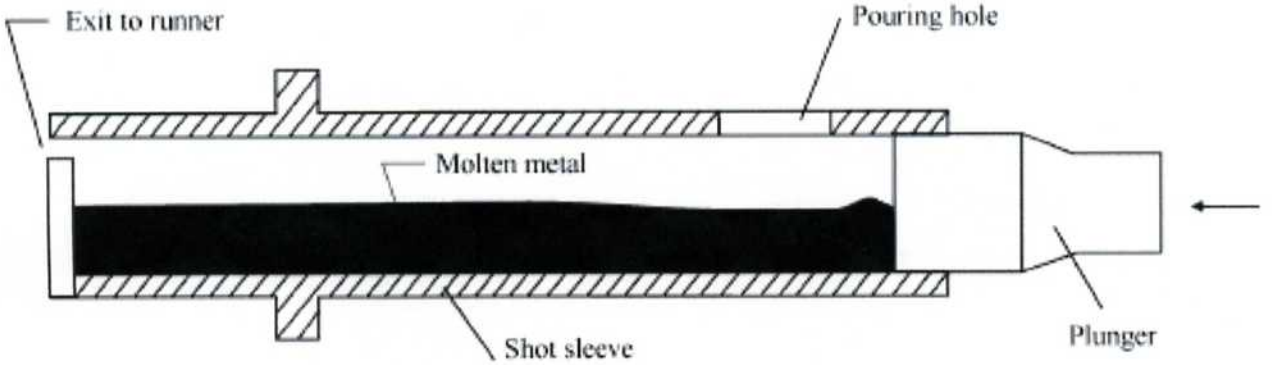

Figure 1 – *Schematic representation of the shot sleeve.*

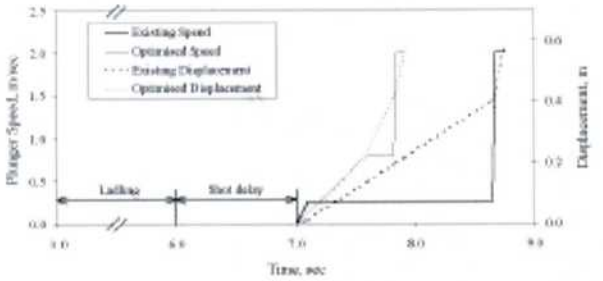

Figure 2 – *The plunger speed and displacement profiles used in this simulation.*

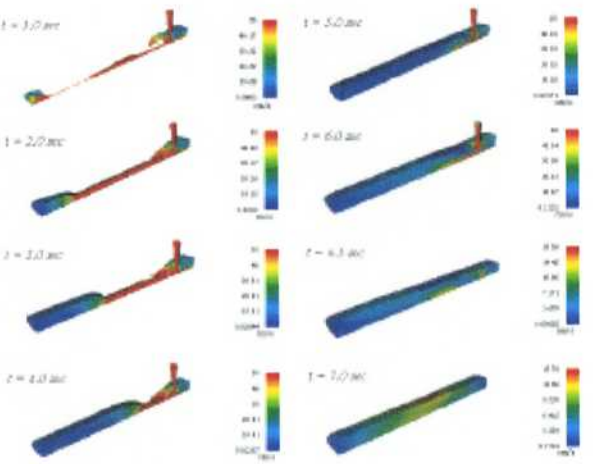

Figure 3 – *Flow pattern during metal pouring into the shot sleeve.*

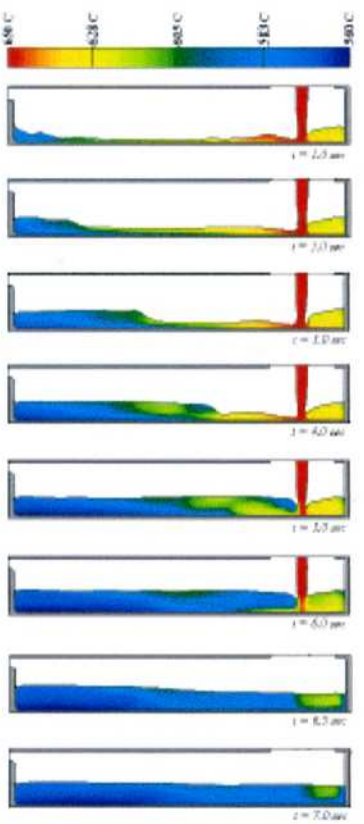

Figure 4 – *2-D view of the temperature distribution and wave formation during ladling.*

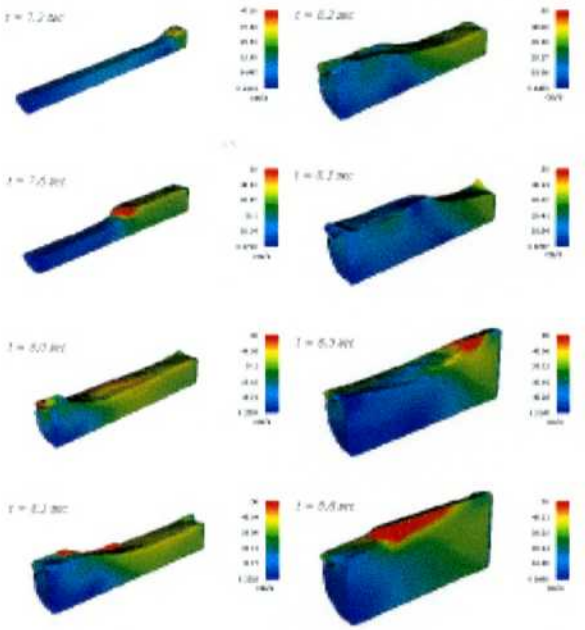

Figure 5 – *3-D view of the flow pattern during plunger advance for the normal plunger parameter set-up.*

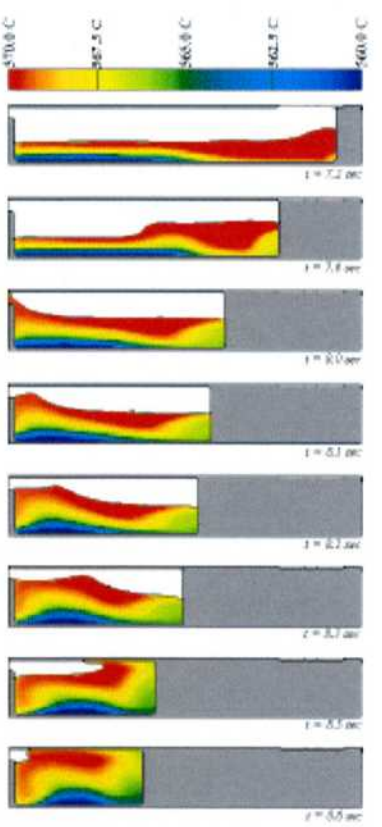

Figure 6 – *2-D view of the temperature distribution and wave front during the plunger advance at first stage with the normal plunger set-up.*

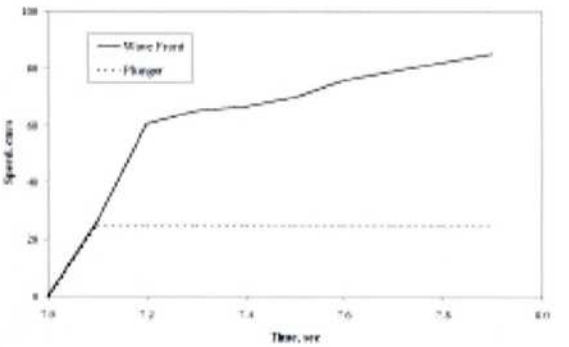

Figure 7 – *The wave speed compared with the plunger speed under the normal condition.*

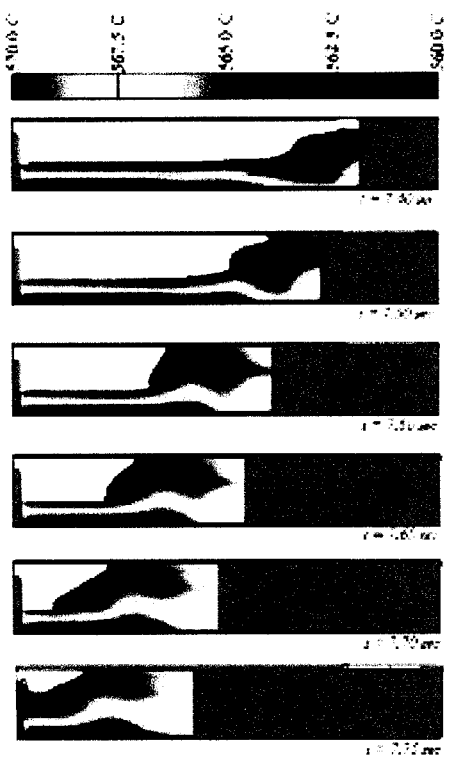

Figure 8 – *2-D view of the temperature distribution and wave front during the plunger advance under the optimized condition.*

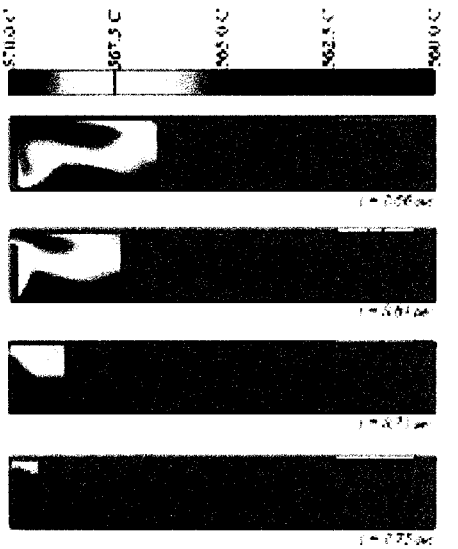

Figure 9 – *2-D view of the temperature distribution during the plunger advance at second stage with normal plunger set-up.*

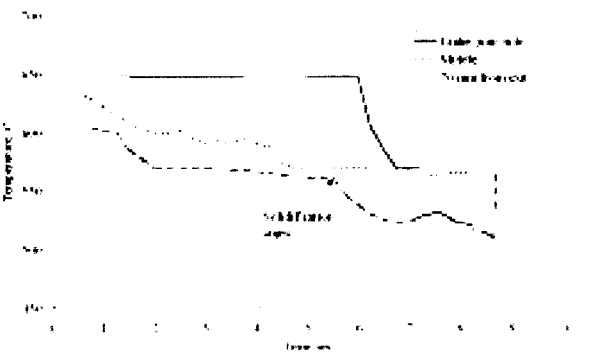

Figure 10 – *The temperature traces at the locations near the bottom face of the shot sleeve under the normal condition.*

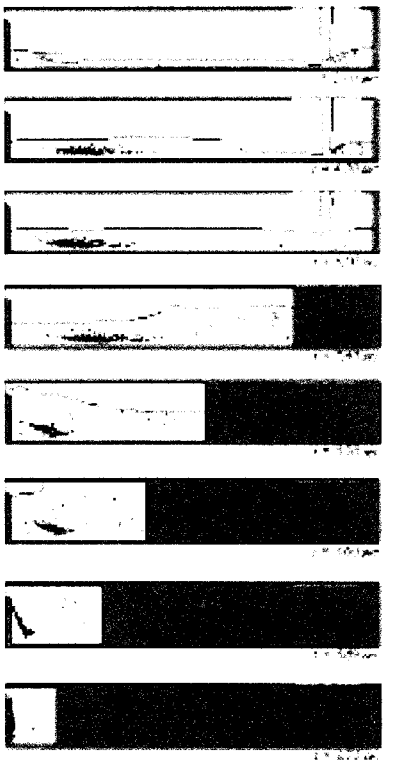

Figure 11 – *The positions of the particles representing the distribution of the first metal into the shot sleeve.*